Int. J. Electrochem. Sci., 17 **(2022)** Article Number: 220629, doi: 10.20964/2022.06.45

International Journal of
ELECTROCHEMICAL
SCIENCE
www.electrochemsci.org

Short Communication

Simultaneous effect of Artificial and natural of pozzolanic materials on corrosion behavior of AISI 1020 carbon steel reinforcing bars embedded in concrete and exposed to 3.5% NaCl

Yu Wang[1], *Zhangfeng Guo*[2], *Hongliang Ge*[1], *Rui Wang*[1,*]

[1] School of Materials and Chemistry, China JiLiang University, Hangzhou 310018, China
[2] China Railway 20th Bureau Group Third Engineering Co., Ltd, Chongqing 400065, China
[*]CorrespondingsE-mail: 3100103159@zju.edu.cn

Received: 3 March 2022 / *Accepted:* 30 March 2022 / *Published:* 7 May 2022

Chloride ions penetrate steel reinforced concrete structures when they are exposed to maritime environments, causing corrosion of the reinforced bars and substantial structural damage. The impact of artificial and natural pozzolans as partial replacements for PC on the concrete strength and electrochemical corrosion activity of AISI 1020 carbon steel rebars was investigated in this study. A 3.5wt% NaCl solution was used to expose steel reinforced concrete specimens. The compressive strength of the PC combined with both volcanic pumice powder (VP) and silica fume from silicon smelting (SFS) increased significantly, according to the mechanical results for concrete examples. Water absorption is considerably decreased in the SV concrete specimen. The SV specimen had a minor passive-current density compared to the other specimens, showing that carbon steel reinforced concrete with both VP and SFS mixtures has enhanced corrosion resistance. In comparison to the other samples, the EIS results demonstrate that the SV specimen has a considerable enhancement in polarization resistance, which indicates a stronger corrosion resistance. SEM analysis of the steel surface revealed that the concrete building, including VP and SFS additives, was more homogeneous and dense than the PC sample, which was in accordance with electrochemical outcomes.

Keywords: Electrochemical corrosion; Artificial and natural of pozzolanic materials; AISI 1020 carbon steel rebars; Corrosive environment

1. INTRODUCTION

Concrete is the world's most widely utilized substance [1-3]. Steel reinforced concrete is now commonly utilized to improve the longevity of concrete structures [4-6]. Building materials, on the other hand, are frequently subjected to corrosive media such as carbonization, coupling effects, freeze-

thaw cycles, and chloride assault, all of which contribute to steel rebar corrosion [7, 8]. Concrete permeability is a flaw in concrete durability because it allows water or other liquids to easily pass through it, carrying corrosive elements with them [9, 10].

The use of pozzolanic elements such as metakaolin and fly ash, both artificial and natural, has been proven to be a useful way of enhancing concrete characteristics [11, 12]. With growing environmental concerns, the use of silica fume from silicon smelting (SFS) as a mixer and alternative additive has gained popularity [13-15]. SFS is a pozzolanic compound with a variety of unique features. It comes in a variety of styles and quality levels. Furthermore, SFS is a well-liked additive for use in cement and concrete [16-18]. SFS is increasingly being utilized to create materials with lower porosity, a denser microstructure, increased ion resistance, increased strength, and durability [19, 20].

As a result, alternative precursor materials have been identified as necessary. In recent research, volcanic pumice powder (VP) has been proposed as a sustainable method of finding alkali-activated material [21]. This is abundantly available in a number of nations, although it is rarely used in particular settings, which has sparked a lot of interest in its use as a forerunner to alkali-activated material [22, 23]. The number of studies utilizing VP-based materials has steadily increased, with the majority of findings focused on mechanical and physical properties and few on durability.

Because no earlier studies of the combined effects of VP and SFS on the corrosion protection of steel reinforced cement has been published. The electrochemical corrosion performance of reinforcing carbon steel in concrete with VP and SFS was considered in this study. Corrosion resistance of AISI 1020 carbon steel rebar was examined through an electrochemical impedance spectroscopy test, polarization consideration, and open-circuit potential assessment.

2. EXPERIMENTAL

The varied components of volcanic pumice powder (VP) and silica fume from silicon smelting (SFS) in Portland cement (PC) were used in this study. Table 1 lists the properties of the VP, SFS, and PC.

Table 1. Chemical compositions of VP, SFS and PC

	PC(wt%)	**VP(wt%)**	**SFS(wt%)**
SiO_2	20.35	51.42	97.23
Al_2O_3	4.74	17.81	0.23
Fe_2O_3	3.32	6.32	0.52
CaO	63.25	6.42	0.21
MgO	3.04	6.15	0.53
K_2O	0.62	3.26	0.51
Na_2O	0.30	5.64	0.11
SO_3	2.95	0.53	0.12
LOI	0.89	0.23	0.54

All mortars were produced with the same ratio of sand to cement (3:1). The SFS and VP were used as partial replacements for PC. The water to cement ratio was 0.47. Table 2 displays the proportions of the blends for each specimen. The mixes were poured into cylinder molds with a diameter of 11cm and a height of 27cm, and then stored at room temperature for one day with a high humidity of 90%.

Table 2. The concrete sample mix proportions

Sample	PC(wt%)	SFS(wt%)	VP(wt%)
Portland cement	100.0	0.0	0.0
SFS	70.0	30.0	0.0
VP	80.0	0.0	30.0
SV	80.0	15.0	15.0

Table 3. AISI 1020 carbon steel reinforcing chemical composition (wt%)

C	Si	Ni	Mn	Cr	P	S	Fe
0.18	0.25	0.11	0.44	0.14	0.0046	0.016	Residual

Electrochemical studies on steel rebar were conducted to investigate the effects of SFS and VP mixtures on the corrosion behavior of carbon steel reinforced concrete. Table 3 exhibits the carbon steel reinforcing chemical composition.

The electrochemical corrosion parameters of the specimens were studied using a three-electrode electrochemical setup. The working, reference, and counter electrodes were made of steel reinforced concrete, conventional copper/copper-sulfate electrode, and graphite. The samples were immersed in a 3.5wt% NaCl media to simulate the marine environment. Using sophisticated software, the resulting results were examined. In the frequency ranges of 100kHz to 0.1mHz, electrochemical impedance spectroscopy (EIS) investigations were performed. The cyclic voltammetry assessment was conducted at a scan rate of 50mV/s between -1.2V and 0.8V. The polarization evaluation was performed at a 1mV/s scanning rate at 0.25V. According to IS 516e1959, compressive strength tests were performed on three specimens for each mixture for one day, one week, two weeks, and four weeks. The morphological properties of rebar were studied using a scanning electron microscope (SEM). Water absorption was measured using ASTM C642.

3. RESULTS AND DISCUSSION

Different admixtures were used to replace PC in carbon steel reinforced concrete. Figure 1 shows the corrosion potential of samples exposed to 3.5 wt% NaCl aqueous solution, representing that the SFS sample has a 10% corrosion probability throughout the duration of the exposure period, with a corrosion potential greater than -200mV [24, 25]. For 1 to 6 weeks, the PC sample showed an unclear

corrosion with potential values of -300 mV to -200 mV vs. CSE, which was connected to the beginning of corrosion damage or a minor separation of the passivation film [26].

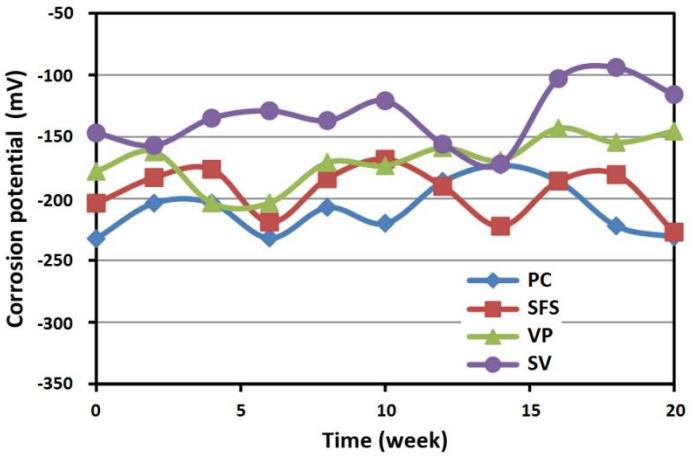

Figure 1. Corrosion potential for steel reinforcement bars in concrete produced by replacing various admixtures for PC into a 3.5wt% Nacl aqueous solution.

The corrosion potential results for the SV specimen were more robust than the other specimens' potential values, which stayed completely within the 10%-corrosion probability zone [27-29]. Because of the decrease in calcium hydroxide, absorption of hydration products, and change in pore solutions, one of the most significant aspects of the VP is its great impact on concrete durability.

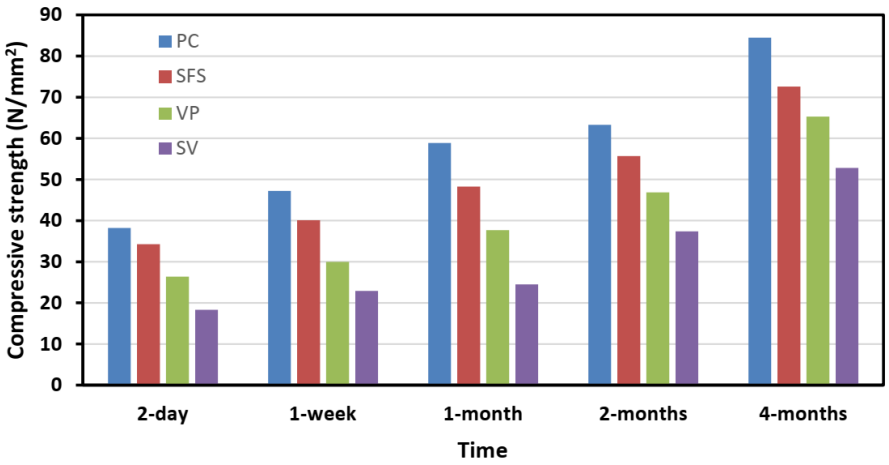

Figure 2. A compressive strength for the specimens at ambient temperature with various replacement combinations

Fig. 2 depicts the compressive strength of the specimen. When the different replacement combinations are compared, it can be determined that the SV sample seems to have a higher strength at every age. The greater concentration of CaO in VP could explain the rise in strength. It acts both

hydraulically and pozzolanically, leading to a high, dense, and pore-structured material [30-32]. In comparison to other specimens, SV mixes were found to have a high strength. Moreover, for each percentage of SFS replacement, concrete containing the SFS had a better starting strength. The overall strength of the concrete was likewise greater than that of the PC concrete.

Figure 3 depicts the polarization curves of steel bars in concrete with various additives after 4 months of exposure to 3.5 wt% NaCl media. All carbon steel bars are examined through passive areas, as revealed in Fig. 3, demonstrating that passive films are generated on the surface of AISI 1020 steel when steel reinforcement bars were exposed to a corrosive environment. Furthermore, a major shift in corrosion-potential forward towards positive-direction was discovered, demonstrating that anodic steel dissolution may be effectively delayed by varying the quantity of additives in concrete structures [33-35].

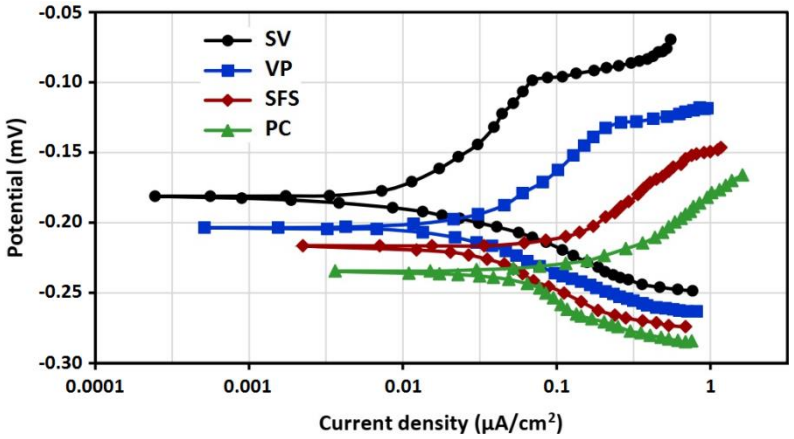

Figure 3. The polarization plots of carbon steel bars in concrete with various additives after 4-month of exposure to3.5 wt% NaCl media

Table 4. Corrosion elements derived from polarization curves shown in Figure 3.

Samples	Current-density(µA/cm^2)	Corrosion-potential(V)	β_a(mVdec^{-1})	β_c(mVdec^{-1})
Portland cement	0.218	-0.235	34	52
SFS	0.078	-0.215	38	55
VP	0.059	-0.203	42	57
SV	0.027	-0.178	47	51

The SV sample has a considerably larger passive zone compared to the other specimens. Additionally, passive-current density in the SV specimen was lower compared to the other specimens, showing that carbon steel rebar in concrete, including both VP and SFS mixtures, has enhanced

corrosion resistance. It's because the VP reacted to free calcium hydroxide during the cement hydration process, making more calcium-silicate-hydrate that developed the mechanical properties and durability of the concrete structures [36-38]. Table 4 displays the corrosion elements derived from the polarization curves in Fig. 3.

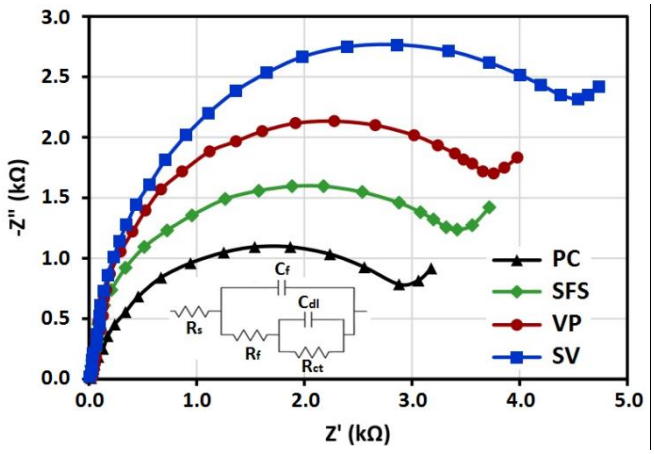

Figure 4. EIS plots made using carbon steel reinforced concrete and various admixtures in a 3.5% NaCl solution. An applied circuit model is shown in the inset.

The corrosion resistance of steel reinforcement bars made with various admixtures in a 3.5% NaCl solution was investigated using the EIS approach. Figure 4 shows the Nyquist plots derived from the EIS study. The analogous circuit employed in this study is shown in the inset of Fig. 4. R_s denotes the resistance to the solution. Capacitance and resistance of covered concrete are represented through C_f and R_f, respectively [39-41]. Charge-transfer resistance and double-capacitance of AISI 1020 steel surfaces are represented by R_{ct} and C_{dl}, respectively [42-44]. Table 5 shows the results of the research.

Table 5. Results obtained with various mixtures in a 3.5% NaCl solution for steel reinforced concrete.

Sample	R_s(Ω)	R_f(kΩ)	R_{ct}(kΩ)	C_f(μF cm^{-2})	C_{dl}(μF cm^{-2})
PC	28.3	2.33	3.32	9.2	11.2
SFS	26.4	3.25	4.64	5.6	8.7
VP	32.8	3.96	5.19	4.1	7.5
SV	30.7	5.17	7.36	3.4	5.2

As shown in table 5, when VP and SFS are replaced with PC, C_f falls and R_f increases, indicating an improvement in the durability and corrosion resistance, as well as the thickness of the passive film on carbon reinforcing steel. The VP causes a pozzolanic reaction via $Ca(OH)_2$, resulting in a homogeneous, insoluble, and dense calcium hydroxide gel [45]. Furthermore, due to its high specific surface area, VP can form a strong bond with hydrated cement, inhibiting Ca(OH)2 $Ca(OH)_2$ formation [46, 47]. Both additives fill in minor cracks and capillary pores, causing the concrete

structure to shrink. In a corrosion environment, these compounds improve the resistance to corrosion of carbon steel rebar.

Figure 5 illustrates the water absorption of concrete structures with different mixtures after being subjected to a 3.5% NaCl aqueous solution for 1-week, 1-month, 2-month, and 4-month. When the exposure period was increased, all of the mixture samples showed a decrease in water absorption when compared to PC samples, as shown in Fig. 5. This means that VP and SFS admixtures in PC could significantly decrease the water absorption of a concrete building after being exposed to a marine environment. Consequently, once both mixtures are employed, the water absorption of samples is reduced.

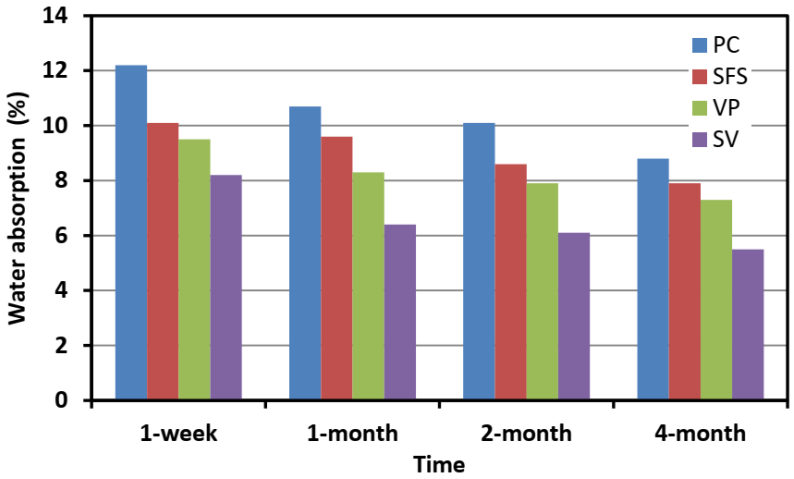

Figure 5. Water absorption for concrete structures with diverse mixtures in a marine environment after varied immersion times

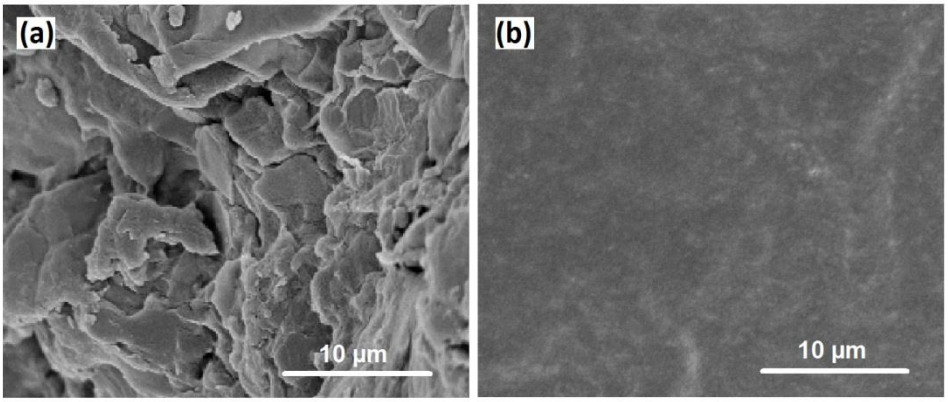

Figure 6. SEM image of steel rebars in various concrete samples after being immersed in a 3.5wt% NaCl environment for 8 weeks.

After eight weeks in the marine environment, Figure 6 displays the surface morphologies of different concrete samples. Low corrosion products and the smallest pits are visible on the surface of the SV specimen, demonstrating minimal pitting corrosion shaped into the surface of AISI 1020 steel rebar, which is consistent with electrochemical studies. This could be linked to chloride ion decreases

and water permeability in reinforced concrete samples. Admixtures can modify the structure of the cement paste by converting large pores to minor pores. The decrease in water permeability and Cl^- ions caused by the addition of VP and SFS mixtures to OPC resulted in a lower corrosion rate and enhanced corrosion protection of AISI 1020 steel rebar.

4. CONCLUSIONS

In this research, the impact of artificial and natural pozzolans as partial replacements for PC on concrete strength and the electrochemical corrosion activity of carbon steel rebars was investigated in this study. A 3.5wt% NaCl solution was used to expose steel reinforced concrete specimens. According to the mechanical results for concrete examples, the compressive strength of the PC combined with both VP and SFS increased significantly. Water absorption is considerably decreased in the SV concrete specimen. The SV specimen had a minor passive-current density compared to the other specimens, showing that carbon steel reinforced concrete with both VP and SFS mixtures has enhanced corrosion resistance. In comparison to the other samples, the EIS results demonstrate that the SV specimen has a considerable enhancement in polarization resistance, which indicates a stronger corrosion resistance. SEM analysis of the steel surface revealed that the concrete building, including VP and SFS additives, was more homogeneous and dense than the PC sample, which was in accordance with electrochemical outcomes.

References

1. H. Huang, M. Huang, W. Zhang and S. Yang, *Structure and infrastructure engineering*, 17 (2021) 1210.
2. H. Huang, C. Xue, W. Zhang and M. Guo, *Engineering Structures*, 251 (2022) 113479.
3. S. Kakooei, H.M. Akil, M. Jamshidi and J. Rouhi, *Construction and Building Materials*, 27 (2012) 73.
4. M. Alexander and H. Beushausen, *Cement and Concrete Research*, 122 (2019) 17.
5. L. Sun, C. Li, C. Zhang, Z. Su and C. Chen, *International Journal of Structural Stability and Dynamics*, 18 (2018) 1840001.
6. K. Tan, Y. Qin, T. Du, L. Li, L. Zhang and J. Wang, *Construction and Building Materials*, 287 (2021) 123078.
7. C.-l. Zhang, W.-k. Chen, S. Mu, B. Šavija and Q.-f. Liu, *Construction and Building Materials*, 285 (2021) 122806.
8. W. Zhang and Z. Tang, *Journal of Composites for Construction*, 25 (2021) 04021043.
9. S. Dey, V. Kumar, K. Goud and S. Basha, *Journal of Building Pathology and Rehabilitation*, 6 (2021) 1.
10. S. Guo, C. Li, Y. Zhang, Y. Wang, B. Li, M. Yang, X. Zhang and G. Liu, *Journal of Cleaner Production*, 140 (2017) 1060.
11. M. Amran, S. Debbarma and T. Ozbakkaloglu, *Construction and Building Materials*, 270 (2021) 121857.
12. Z. Wu, S. Wu, J. Bao, W. Qian, S. Karabal, W. Sun and P.J. Withers, *International Journal of Fatigue*, 151 (2021) 106317.
13. O.Y. Bayraktar, *Environmental Science and Pollution Research*, 28 (2021) 16843.

14. M. Yang, C. Li, Y. Zhang, D. Jia, R. Li, Y. Hou, H. Cao and J. Wang, *Ceramics International*, 45 (2019) 14908.
15. Y.-M. Chu, U. Nazir, M. Sohail, M.M. Selim and J.-R. Lee, *Fractal and Fractional*, 5 (2021) 119.
16. Y. Wang, H. Zhou and Y. Zhang, *International Journal of Electrochemical Science*, 15 (2020) 3232.
17. J. Zhang, C. Li, Y. Zhang, M. Yang, D. Jia, G. Liu, Y. Hou, R. Li, N. Zhang and Q. Wu, *Journal of cleaner production*, 193 (2018) 236.
18. S. Kakooei, H.M. Akil, A. Dolati and J. Rouhi, *Construction and Building Materials*, 35 (2012) 564.
19. T. Wu, X. Yang, H. Wei and X. Liu, *Construction and Building Materials*, 199 (2019) 526.
20. F. Chen, Z. Jin, E. Wang, L. Wang, Y. Jiang, P. Guo, X. Gao and X. He, *Scientific Reports*, 11 (2021) 1.
21. Q. Tran and P. Ghosh, *Construction and building materials*, 249 (2020) 118741.
22. C. Zhang and F. Zhang, *International Journal of Electrochemical Science*, 15 (2020) 3740.
23. M. Nazeer, F. Hussain, M.I. Khan, E.R. El-Zahar, Y.-M. Chu and M. Malik, *Applied Mathematics and Computation*, 420 (2022) 126868.
24. A.S. AL-Ameeri, M.I. Rafiq and O. Tsioulou, *Cement and Concrete Composites*, 115 (2021) 103819.
25. W. Liu, Z. Guo, C. Wang and S. Niu, *Construction and Building Materials*, 299 (2021) 124011.
26. Y. Zhang, B. Hinton, F.B. Varela, M. Forsyth and M.Y. Tan, *Corrosion Engineering, Science and Technology*, 53 (2018) 517.
27. V.A. Franco-Luján, M.A. Maldonado-García, J.M. Mendoza-Rangel and P. Montes-Garcia, *Construction and Building Materials*, 198 (2019) 608.
28. Y. Zhang, H.N. Li, C. Li, C. Huang, H.M. Ali, X. Xu, C. Mao, W. Ding, X. Cui and M. Yang, *Friction*, (2022) 1.
29. N. Naderi, M. Hashim, J. Rouhi and H. Mahmodi, *Materials science in semiconductor processing*, 16 (2013) 542.
30. B. Rolón and P.F. Castañeda, *Cleaner Materials*, 2 (2021) 100028.
31. M. Wang, X. Yang and W. Wang, *Construction and Building Materials*, 315 (2022) 125740.
32. Y.-M. Chu, B. Shankaralingappa, B. Gireesha, F. Alzahrani, M.I. Khan and S.U. Khan, *Applied Mathematics and Computation*, 419 (2022) 126883.
33. R. Combrinck, M. Kayondo, B. Le Roux, W. De Villiers and W. Boshoff, *Construction and Building Materials*, 202 (2019) 139.
34. M. Rahimi-Golkhandana, S. Danesha and A. Davoodib, *Water Conservation and Management* 5(2021) 78.
35. C. Xin, L. Changhe, D. Wenfeng, C. Yun, M. Cong, X. Xuefeng, L. Bo, W. Dazhong, H.N. LI and Y. ZHANG, *Chinese Journal of Aeronautics*, (2021) 1.
36. Y. Liang, *Chemical Physics Letters*, 761 (2020) 138117.
37. K. Zhou, J. Xu, G. Xiao and Y. Huang, *Journal of Materials Processing Technology*, 302 (2022) 117503.
38. M. Liu, C. Li, Y. Zhang, Q. An, M. Yang, T. Gao, C. Mao, B. Liu, H. Cao and X. Xu, *Frontiers of Mechanical Engineering*, 16 (2021) 649.
39. G. Zhao, S. Wen and X. Sun, *International Journal of Electrochemical Science*, 16 (2021) 1.
40. X. Wu, C. Li, Z. Zhou, X. Nie, Y. Chen, Y. Zhang, H. Cao, B. Liu, N. Zhang and Z. Said, *The International Journal of Advanced Manufacturing Technology*, 117 (2021) 2565.
41. T.H. Zhao, M.I. Khan and Y.M. Chu, *Mathematical Methods in the Applied Sciences*, (2021) 1.
42. P. Divya, S. Subhashini, A. Prithiba and R. Rajalakshmi, *Materials Today: Proceedings*, 18 (2019) 1581.

43. T. Shi, Y. Lan, Z. Hu, H. Wang, J. Xu and B. Zheng, *International Journal of Concrete Structures and Materials*, 16 (2022) 1.
44. R. Mohamed, J. Rouhi, M.F. Malek and A.S. Ismail, *International Journal of Electrochemical Science*, 11 (2016) 2197.
45. A.V. Korkmaz, *Case Studies in Construction Materials*, 16 (2022) e00868.
46. A.D. Çavdar, H. Yel and S.B. Torun, *Journal of Building Engineering*, 48 (2022) 103975.
47. A. Abetua and A. Kebedeb, *Water Conservation and Management*, 2 (2021) 40.